J Mater Sci (2011) 46:1337–1340
DOI 10.1007/s10853-010-4924-3

Hydrothermal synthesis and photoluminescence properties of $Y_2Zr_2O_7:Tb^{3+}$ phosphors

Linhui Gao · Yue An · Hongliang Zhu · Lun Wang · Jianjun Chen · Naiyan Wang · Guofu Ou

Received: 31 March 2010 / Accepted: 13 September 2010 / Published online: 25 September 2010

Abstract This article presents the synthesis and photoluminescence (PL) properties of $Y_2Zr_2O_7:Tb^{3+}$. The Tb^{3+}-doped $Y_2Zr_2O_7$ zirconates were successfully synthesized by a hydrothermal process at 200 °C for 20 h. X-ray diffractometer (XRD) patterns revealed that all of the products were phase-pure with the fluorite structure. PL study showed that the $Y_2Zr_2O_7:Tb^{3+}$ phosphors exhibited obvious PL emission peaks which located at 490, 545, 585, and 623 nm; the dominant emission located at 545 nm is assigned to $^5D_4 \rightarrow {}^7F_5$ transition. Furthermore, Tb^{3+}-doping concentration strongly affected the PL properties, and the quenching concentration is 5 at.%.

Introduction

The rare-earth zirconates with the formula $Re_2Zr_2O_7$ are of great interest for many researchers over a number of years. There are a variety of actual and potential applications for these materials used as thermal barrier coatings [1], catalysts [2], nuclear waste forms [3], solid electrolytes [4], and phosphors [5]. These materials have many advantages such as low thermal conductivity, high melting point, high thermal expansion coefficient, high stability and ability to accommodate defects. In recent years, the rare-earth zirconates phosphors have captured much attention due to their potential application as a new kind of phosphors. Therefore, research on the synthesis and luminescence properties is of great interest in scientific community.

Up to now, variety of synthesis methods regarding developing rare-earth zirconates have been proposed, including conventional solid-state reaction, sol–gel, combustion, stearic acid method, and hydrothermal. In general, the high temperature solid-state is still the most commonly synthetic method. This synthesis route employs a solid-state reaction of ZrO_2 with appropriate rare-earth oxides at high temperature more than 1200 °C for a long time (several days), which produce large agglomerates and must be ground or milled to obtain a fine powder. This process greatly decreases the luminescence efficiency and changes the original morphology. To avoid high preparation temperatures and agglomerations of fine powders, lots of methods have been adopted. Tong et al. [2] successfully synthesized fluorite type $Y_2Zr_2O_7$ nanocrystals by stearic acid method. And found that the preparation temperature was lowered and the reaction time was shortened by this method. Zhang et al. [6, 7] synthesized a series of $Re_2Zr_2O_7$ (RE = La, Nd, Eu, and Y) nanopowders by a sol–gel–combustion route and found it need neither high heating temperature nor long calcination time. Photoluminescence (PL) in the UV and visible range can be observed from these materials, but they only studied the luminescence properties of Pb-ion-doped rare-earth zirconates.

L. Gao · H. Zhu · L. Wang · J. Chen · N. Wang
Center of Materials Engineering, Zhejiang Sci-Tech University, Xiasha University Town, Hangzhou 310018, People's Republic of China

L. Gao
Key Laboratory of Advanced Textile Materials and Manufacturing Technology, Zhejiang Sci-Tech University, Hangzhou 310018, People's Republic of China
e-mail: glinhui@hotmail.com

Y. An
Department of Chemical and Biological Engineering, Zhejiang University, Hangzhou 310027, People's Republic of China

G. Ou (✉)
Lab of Multiphase Flow Erosion & Deposition, Zhejiang Sci-Tech University, Xiasha University Town, Hangzhou 310018, People's Republic of China
e-mail: ougf@163.com

Furthermore, they used the same method synthesized Eu^{3+}-doped $Y_2Zr_2O_7$ nanocrystals. In their work, Eu^{3+} was successfully introduced into the host, and intense multi-band red luminescence of Eu^{3+} has been obtained in $Y_2Zr_2O_7$ matrix. However, the synthesis temperature is still high, at least 600 °C.

In contrast to the above-mentioned methods, hydrothermal synthesis is much simpler, more practical, and more cost-effective. Furthermore, the products prepared by hydrothermal method are of higher chemical homogeneity, more stoichiometric [8, 9]. In this article, we present the hydrothermal synthesis, characterization, and PL property of Tb^{3+}-ion-doped $Y_2Zr_2O_7$ phosphors for the first time. Furthermore, the hydrothermal method presented here may be desirable for the synthesis of other rare-earth zirconates.

Experimental procedures

Yttrium nitrate ($Y(NO_3)_3{\cdot}6H_2O$), terbium nitrate ($Tb(NO_3)_3{\cdot}6H_2O$), zirconium oxychloride hydrate ($ZrOCl_2{\cdot}8H_2O$), and ammonia aqueous solution were used as the starting materials. All the reagents were of analytical grade and used without further purification. The preparation conditions of the $Y_2Zr_2O_7$:Tb^{3+} (Y: Tb = 100:0, 99:1, 97:3, 96:4, 95:5, 94:6, and 93:7, in molar ratio) were similar, so we take $(Y_{0.95}Tb_{0.05})_2Zr_2O_7$ as an example to describe the detailed procedures. First, 1.1490 g of $Y(NO_3)_3{\cdot}6H_2O$ and 0.0715 g of $Tb(NO_3)_3{\cdot}6H_2O$ were added to 40-mL deionized water under vigorous magnetic stirring. Secondly, 1.0180 g of $ZrOCl_2{\cdot}8H_2O$ was added into the other 40-mL deionized water. Then the two kinds of solutions were mixed together by slowly dropping the $ZrOCl_2$ solution into the former. After 15 min stirring, the requisite amount of ammonia solution was added to the mixed solution to adjust pH value of the solution to be 9. The above solution was transferred into a Teflon-lined stainless-steel autoclave (capacity 100 mL) and sealed. The autoclave was heated at 200 °C for 20 h and cooled naturally to room temperature. Finally, the product was collected by centrifugation, washed with deionized water and alcohol several times, and dried at 80 °C for 24 h in air. For comparison, bulk $(Y_{0.95}Tb_{0.05})_2Zr_2O_7$ was obtained by direct solid-state reaction (SR) from the mixture of Y_2O_3, Tb_4O_7, ZrO_2 at 1000 °C for 10 h in air.

Phase identification of the products was carried out by X-ray diffractometer (XRD, Thermo ARL XTRA, Thermo ARL Corp., Dearborn, MI) over a 2θ range from 10° to 80° at a scanning rate of 5°/min. The morphologies of the powders were observed by field-emission scanning electron microscopy (Hitachi S-4800, Japan). The PL emission spectra were obtained on a Hitachi FL4600 fluorescence spectrometer at room temperature. The inductively coupled plasma (ICP) was used to check the rare-earth ions concentration in the solid products.

Results and discussion

The crystallinity and phase purity of the as-prepared samples were characterized by XRD. Figure 1 shows X-ray diffraction (XRD) patterns of the $(Y_{1-x}Tb_x)_2Zr_2O_7$ ($x = 0$, 0.01, 0.03, 0.04, 0.05, 0.06, and 0.07) samples. The four main peaks (111), (200), (220), and (311) are in agreement with the formation of fluorite structure (JCPDS 78-1299) [7, 10, 11], though the JPCDS dates corresponding to $Y_2Zr_2O_7$ phase are still not available for comparison. Figure 2 shows the Tb^{3+} concentration dependence of the lattice parameter. It can be seen that lattice parameter is a linear function of Tb^{3+} concentration, and with the Tb^{3+} concentration increases, the lattice parameter increases. The result showed that the lattice parameter is in good agreement with the rule of lattice selection and ionic radius. The enlarged lattice parameter proves that Tb^{3+} ion in $Y_2Zr_2O_7$:Tb^{3+} replaces Y^{3+} ion because of the larger radius of Tb^{3+} ion than that of Y^{3+} ion. The results demonstrate that the product is phase pure, and no different phase is detected even at a high Tb^{3+} concentration (7 at.%). To confirm neither Y nor Tb components used for the reaction remain in the solution phase in the reaction mixture, we added appropriate amount of NaOH solution into the solution by adjust pH value to be 12, and didn't find any cloudy white precipitation, which implied that no rare-earth ions is still in the solution. Moreover, the Y and Tb concentration in final products was checked using analysis of ICP method, which shows good agreement with calculation. Obviously,

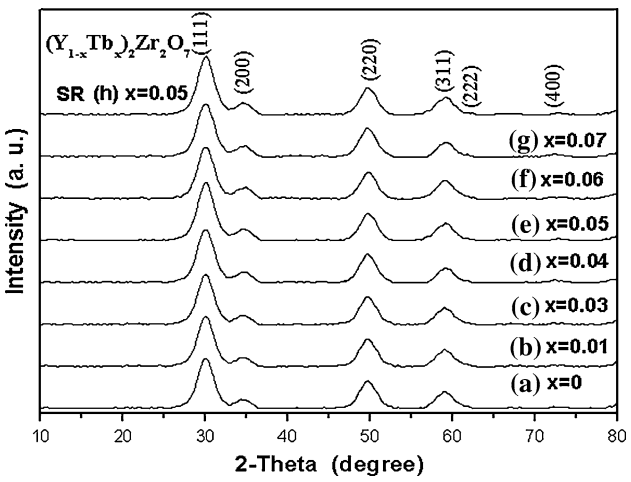

Fig. 1 XRD patterns of $(Y_{1-x}Tb_x)_2Zr_2O_7$ particles: (*a*) $x = 0$, (*b*) $x = 0.01$, (*c*) $x = 0.03$, (*d*) $x = 0.04$, (*e*) $x = 0.05$, (*f*) $x = 0.06$, (*g*) $x = 0.07$, and (*h*) $x = 0.05$(SR)

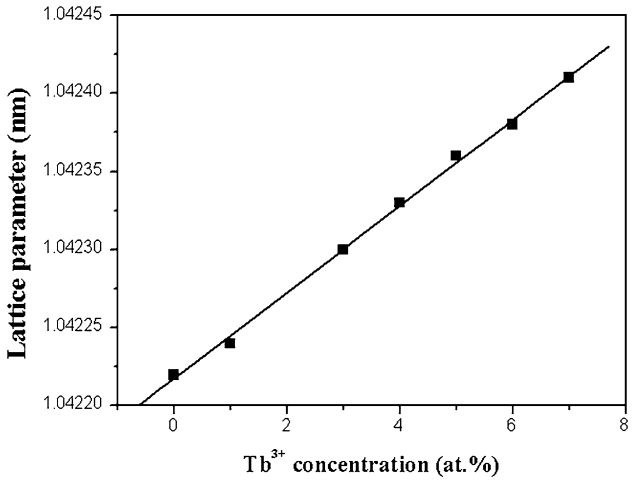

Fig. 2 Lattice parameter as a function of Tb^{3+} concentration

all the amounts of the chemicals used formed a solid phase in the hydrothermal process.

Figure 3 is the field emission scanning electron microscopy (FE-SEM) image of $Y_2Zr_2O_7$:Tb^{3+} (5%) synthesized by the hydrothermal and SR process, respectively. Figure 3a exhibits the low-magnification FE-SEM image of the as-synthesized $Y_2Zr_2O_7$:Tb^{3+} morphology which demonstrates that the product is mainly straight rods and some random dispersed particles. The morphology of high-magnification, as shown in Fig. 3b, clearly exhibits that the main particles are nano-rods and some random dispersed nano-particles. The width of the nano-rod is 50 nm on average and the length is range from 400 to 1000 nm. The morphology and particle sizes of other Tb^{3+}-doped phosphors synthesized by hydrothermal method in this study are almost the same as $(Y_{0.95}Tb_{0.05})_2Zr_2O_7$. Compared with the product of SR (as shown in Fig. 3c), the particle size of hydrothermal synthesized gets smaller and the surface of the product is relatively smoother. Rare-earth oxide and hydroxide materials have been proven can be easily rolled into nanorods and nanotubes under a hydrothermal process at relatively high temperature and pressure using NaOH or ammonia as mineralizer.

The PL property of the $Y_2Zr_2O_7$:Tb^{3+} phosphor was investigated by fluorescence spectrophotometer. Figure 4 shows the typical PL excitation spectra of $(Y_{0.95}Tb_{0.05})_2Zr_2O_7$ obtained by hydrothermal method. The excitation spectrum obtained by monitoring the emission of $^5D_4 \rightarrow {}^7F_5$ (545 nm) consists of an intense broadband centered at 245 nm, which is assigned to the f–d transition of Tb^{3+} in the excitation [12].

Figure 5 shows the emission spectra of $(Y_{1-x}Tb_x)_2Zr_2O_7$ ($x = 0.01$, 0.03, 0.04, 0.05, 0.06, and 0.07) and the emission spectra of SR. As can be seen, the emission spectrum consists of intensive PL emission in the spectral range of 450–650 nm under 254-nm excitation. The main emission peaks at 490, 545, 585, and 623 nm were, respectively, assigned to the $^5D_4 \rightarrow {}^7F_6$, $^5D_4 \rightarrow {}^7F_5$, $^5D_4 \rightarrow {}^7F_4$, and $^5D_4 \rightarrow {}^7F_3$ transitions of Tb^{3+} [13]. The dominant peak is the green emission of 545 nm. Tb^{3+}-doped phosphors have been extensively utilized in display devices owing to their intense green emission of ~545 nm. The predominant green emission implies the $Y_2Zr_2O_7$:Tb^{3+} phosphors can be used as a potential luminescence material. Furthermore, from the inset, it can be seen that there existed a concentration quenching in hydrothermal synthesized samples. The concentration quenching occurred when Tb^{3+} ion is about 5 at.%. When the Tb^{3+} concentration increases to a limited level, the distance between two Tb^{3+} ions decreases, so the energy transfer between each Tb^{3+} ions becomes easier, which leads to the energy transfer between the Tb^{3+} ions become predominant by the non-radiation transitions. Therefore, the emission intensity decreases sharply. The similar emission curve is obtained for the phosphor prepared by SR, but the emission intensity of phosphor prepared by hydrothermal method, in the same doped concentration, is higher than that of phosphor prepared by SR. Generally, it is known that the PL properties of particles are impacted by many factors, such as morphology, size, size distribution, and so on. The lower emission intensity may ascribe to the phosphor prepared by SR had more surface defects. Therefore, the hydrothermal method is promising for synthesis of

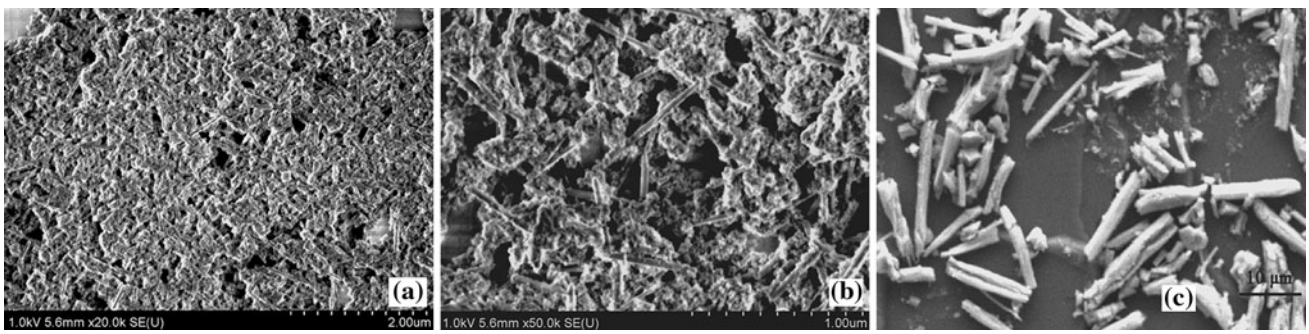

Fig. 3 FE-SEM images of $(Y_{0.95}Tb_{0.05})_2Zr_2O_7$: **a**, **b** low and high magnification prepared by hydrothermal method, **c** prepared by SR

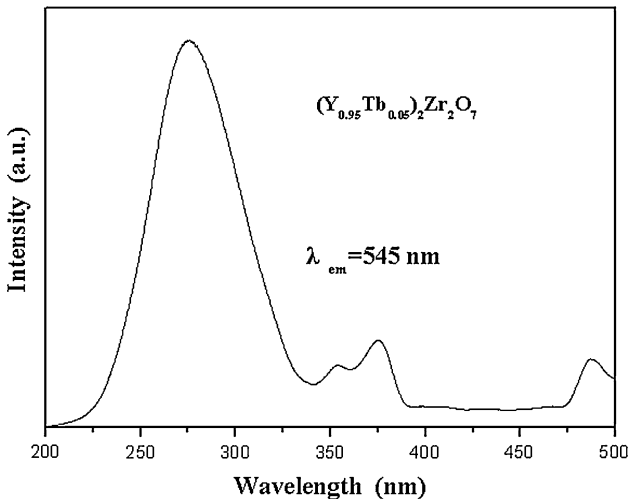

Fig. 4 Photoluminescence excitation spectra of the $(Y_{0.95}Tb_{0.05})_2Zr_2O_7$

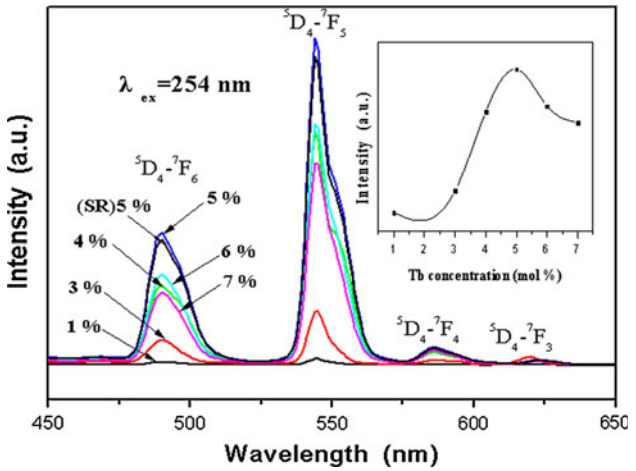

Fig. 5 Photoluminescence emission spectra of the $(Y_{1-x}Tb_x)_2Zr_2O_7$ ($x = 0.01, 0.03, 0.04, 0.05, 0.06$, and 0.07). The *inset* is the change of PL intensity of the $^5D_4 \rightarrow {}^7F_5$ emission with the doping concentration of hydrothermal synthesized samples

rare-earth zirconate phosphors. To further understand the PL property, the decay curve of the $^5D_4 \rightarrow {}^7F_5$ transition of Tb^{3+}-ion-doped $(Y_{0.95}Tb_{0.05})_2Zr_2O_7$ was measured as shown in Fig. 6. It can be well fitted by single exponential equation. The decay time is 2.128 ms, which is short and suitable for PDP application.

Conclusions

In summary, the Tb^{3+}-doped yttrium zirconate ($Y_2Zr_2O_7$:Tb^{3+}) phosphors can be prepared by a mild hydrothermal method at 200 °C for 20 h, and Tb^{3+} ions have been introduced into this host. As the doping level increasing, an obvious concentration quenching is

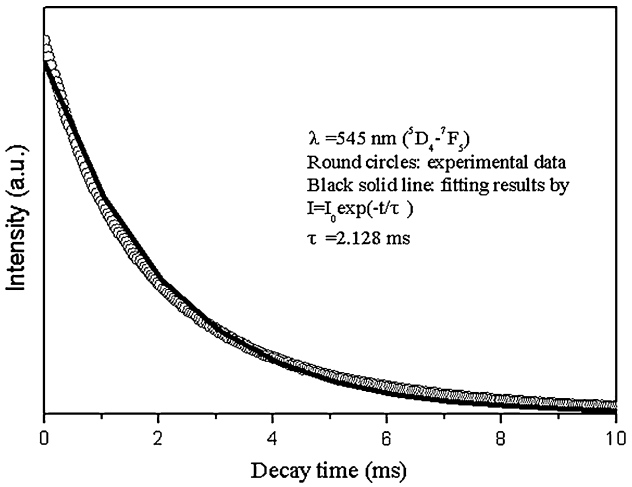

Fig. 6 The decay curve of the $^5D_4$-$^7F_5$ emission of Tb^{3+} in $(Y_{0.95}Tb_{0.05})_2Zr_2O_7$

observed, and the optimum concentration for Tb^{3+} was determined to be about 5 at.%. The PL results showed that the green emission at 545 nm ($^5D_4 \rightarrow {}^7F_5$) is dominant among these peaks.

Acknowledgements This work was supported by the National High Technology Research and Development Program of China (2007AA05Z112), the NSFC (50901068), the ZJNSF (Y4090495), the Foundation of Zhejiang Educational committee (No.20070381), and the Foundation of Key Laboratory of Advanced Textile Materials and Manufacturing Technology (ZSTU) (2006QN04).

References

1. Vassen R, Cao X, Tietz F, Basu D, Stover D (2000) J Am Ceram Soc 83:2023
2. Tong YP, Xue PP, Jian FF, Lu LD, Wang X, Yang XJ (2008) Mater Sci Eng B 150:194
3. Sickafus KE, Minervini L, Grimes RW, Valdez JA, Ishimaru M, Li F, McClellan KJ, Hartmann T (2000) Science 289:748
4. Moreno KJ, Guevara MA, Fuentes AF (2006) J Solid State Chem 179:928
5. Zhang AY, Lü M, Yang ZS, Zhou GJ, Zhou YY (2006) J Phys Chem Solids 67:2434
6. Zhang AY, Lü M, Yang ZS, Zhou GJ, Zhou YY (2008) Solid State Sci 10:81
7. Zhang AY, Lü M, Yang ZS, Zhou GJ, Zhou YY (2008) Mater Chem Phys 109:108
8. Zhu HL, Yang DR, Zhu LM, Li DS, Chen PH, Yu GX (2007) J Am Ceram Soc 90:3095
9. Zhong S, Wang S, Xu H, Hou H, Wen Z, Li P, Wang S, Xu R (2009) J Mater Sci 44:3687. doi:10.1007/s10853-009-3493-9
10. Dhas NA, Patil KC (1993) J Mater Chem 3:1290
11. Yamamura H, Nishino H, Kakinuma K (2008) J Phys Chem Solids 69:1713
12. Li ZH, Zeng JH, Chen C, Li YD (2006) J Cryst Growth 286:493
13. Du N, Zhang H, Ma XY, Li DS, Yang DR (2009) Mater Lett 63:1180